Pharm Res (2014) 31:742–753
DOI 10.1007/s11095-013-1195-0

RESEARCH PAPER

The Effect of Glutathione as Chain Transfer Agent in PNIPAAm-Based Thermo-responsive Hydrogels for Controlled Release of Proteins

Pawel W. Drapala • Bin Jiang • Yu-Chieh Chiu • William F. Mieler • Eric M. Brey • Jennifer J. Kang-Mieler • Victor H. Pérez-Luna

Received: 12 April 2013 / Accepted: 21 August 2013 / Published online: 11 September 2013
© Springer Science+Business Media New York 2013

ABSTRACT

Purpose To control degradation and protein release using thermo-responsive hydrogels for localized delivery of anti-angiogenic proteins.

Methods Thermo-responsive hydrogels derived from N-isopropylacrylamide (NIPAAm) and crosslinked with poly(ethylene glycol)-co-(L-lactic acid) diacrylate (Acry-PLLA-*b*-PEG-*b*-PLLA-Acry) were synthesized *via* free radical polymerization in the presence of glutathione, a chain transfer agent (CTA) added to modulate their degradation and release properties. Immunoglobulin G (IgG) and the recombinant proteins Avastin® and Lucentis® were encapsulated in these hydrogels and their release was studied.

Results The encapsulation efficiency of IgG was high (75–87%) and decreased with CTA concentration. The transition temperature of these hydrogels was below physiological temperature, which is important for minimally invasive therapies involving these materials. The toxicity from unreacted monomers and free radical initiators was eliminated with a minimum of three buffer extractions. Addition of CTA accelerated degradation and resulted in complete protein release. Glutathione caused the degradation products to become solubilized even at 37°C. Hydrogels prepared without glutathione did not disintegrate nor released protein completely after 3 weeks at 37°C. PEGylation of IgG postponed the burst release effect. Avastin® and Lucentis® released from degraded hydrogels retained their biological activity.

Conclusions These systems offer a promising platform for the localized delivery of proteins.

KEY WORDS chain transfer agent · controlled release · immunoglobulin G · PEGylation · thermo-responsive hydrogels

ABBREVIATIONS

Acry-PEG-SVA	Acryloyl-(ethylene glycol)-succinimidyl valerate
Acry-PLLA-*b*-PEG-*b*-PLLA-Acry	Poly(ethylene glycol)-co-(L-lactic acid) diacrylate
AMD	Age related macular degeneration
APS	Ammonium persulfate
BME	β-mercaptoethanol
CTA	Chain transfer agent
DCM	Dichloromethane
EDTA	Ethylenediaminetetraacetic acid
IgG	Immunoglobulin G
LCST	Lower critical solution temperature
NIPAAm	N-isopropylacrylamide
PEG	Poly(ethylene glycol)
PLLA	Poly(L-lactic acid)
PNIPAAm	Poly(N-isopropylacrylamide)
TEA	Triethylamine
TEMED	N,N,N′,N′-tetramethylethylenediamine
VPTT	Volume phase transition temperature

Electronic supplementary material The online version of this article (doi:10.1007/s11095-013-1195-0) contains supplementary material, which is available to authorized users.

P. W. Drapala • V. H. Pérez-Luna (✉)
Department of Chemical and Biological Engineering,
Illinois Institute of Technology
10 West 33rd Street, Chicago, Illinois 60616-3793, USA
e-mail: perezluna@iit.edu

B. Jiang • Y.-C. Chiu • E. M. Brey • J. J. Kang-Mieler
Department of Biomedical Engineering
Illinois Institute of Technology, Chicago, Illinois, USA

E. M. Brey
Department of Research, Hines V.A. Hospital, Hines, Illinois, USA

W. F. Mieler
Department of Ophthalmology and Visual Sciences,
University of Illinois at Chicago, Chicago, Illinois, USA

INTRODUCTION

Hydrogels are useful materials in biomedical applications because their high water content helps preserve the activity of encapsulated biomolecules. They have been extensively investigated for minimally-invasive applications in drug delivery and can be formed under mild conditions of pH and temperature (1–4). This makes them ideal for encapsulation of cells and proteins. Controlled release of molecules from hydrogels can be accomplished using degradable crosslinkers (5,6). Upon degradation of crosslinks the "mesh size" or molecular weight between crosslinks increases, allowing the entrapped biomolecules to diffuse out of the hydrogels.

Stimuli-responsive hydrogels have great potential for drug delivery. They utilize environmental triggers, such as temperature or pH, to effect a change in hydrogel swelling (7–9). Thermoresponsive hydrogels such as poly(N-isopropylacrylamide) (PNIPAAm) are attractive for minimally invasive applications. PNIPAAm exhibits a sharp coil-to-globule phase transition at 32°C, which makes it convenient for drug delivery applications because its transition temperature is between physiological and room temperatures (10). PNIPAAm based hydrogels can be injected through a needle at room temperature so that, when reaching body temperature, they solidify at the site of injection and provide localized drug delivery.

Despite the great potential of PNIPAAm for localized drug delivery there are factors that need to be addressed in order to use it in clinical applications. Some of these are: 1) controlled degradation of the hydrogel so that entrapped molecules can be released over time; 2) control over the "burst" release of molecules; 3) biocompatibility of the hydrogel and its degradation products. In this work hydrogels based on PNIPAAm and cross-linked with a hydrolytically biodegradable crosslinker based on polyethylene glycol (PEG) were used for controlled release of proteins.

The encapsulation and release of IgG and the anti-angiogenic molecules Avastin® and Lucentis® were studied. Avastin® (also known as bevacizumab) and Lucentis® (ranibizumab) are two important anti-angiogenic molecules that have been used for the treatment of the wet form of Age Related Macular Degeneration (AMD) (11–14). Because of their use in the treatment of AMD, the encapsulation of Avastin® and Lucentis® in a drug delivery system that is injectable; degradable; allows controlling the burst release regime, and can be implemented for localized drug release in the eye is of great importance in treatment of AMD.

PNIPAAm hydrogels are biocompatible when implanted in the eye (15). Thus, they are ideal for advancing therapies for the treatment of AMD provided they can be engineered so that burst release can be controlled and the degradation products can be solubilized after degradation. In order to achieve these objectives, two novel methods are used here: (a) PEGylation and tethering of the encapsulated IgG molecules to the degrading polymer chains in order to control initial burst release, and (b) addition of chain transfer agents (CTA) to the hydrogel precursor solution (which would limit the size of polymer chains, facilitating clearance of the degradation products from the body). Glutathione was selected as the CTA because it is a naturally occurring nontoxic antioxidant (16). Addition of glutathione to the hydrogel precursors lowers the size of PNIPAAm chains during polymerization. This can facilitate the clearance of degradation products since it has been shown that PNIPAAm chains smaller than 32 kDa can be eliminated through renal clearance in rats (17). As shown in this work, the use of glutathione as CTA allows controlling the chemistry of thermo-responsive hydrogels in such a way that, when the hydrogel is degraded, the transition temperature of the degraded chains increases above body temperature. This facilitates not only their degradation but also their clearance, which is important for addressing the potential bioaccumulation of hydrogel based drug delivery systems.

MATERIALS AND METHODS

Materials

Unless otherwise stated, all chemicals and materials were used as received and purchased from Sigma-Aldrich (St. Louis, MO). Iodine-125 was from PerkinElmer, Inc. (Waltham, MA). Polystyrene N-chloro-benzenesulfonamide iodination beads (1/8 in. diameter iodination-beads), Trypsin/EDTA (0.05%), Tris-HEPES-SDS running buffer and dialysis cartridges (10 kDa MW cut-off) were from Fisher Scientific (Waltham, MA). MTS Assay Kit was obtained from Promega Corporation (Madison, WI). Bromodeoxyuridine (BrdU) enzyme-linked immuno sorbent assay (ELISA) kit was from CalBiochem (San Diego, CA). Dulbecco's Modified Eagle's Medium (DMEM), Dulbecco's phosphate buffered saline (DPBS; 10X), Hanks' balanced salt solution (HBSS), fetal bovine serum (FBS) and sodium bicarbonate (7.5% w/v) solution were from Cellgro (Manassas, VA). Fibronectin and penicillin/streptomycin were from Invitrogen Corporation (Carlsbad, CA). Avastin® and Lucentis® were from Genentech, Inc. (San Francisco, CA). Acrylate-PEG-succinimidyl valerate PEGylation reagent (Acry-PEG-SVA; MW = 3,400) was from Laysan Bio, Inc. (Arab, AL). Ready-precast electrophoresis gels (polyacrylamide gel), laemmli sample buffer (laemmli), SDS-PAGE standards (45–200 kDa) and 2-mercaptoethanol (98.0%) were from Bio Rad Laboratories Inc. (Hercules, CA). Coomassie protein stain was from Carolina Biological (Burlington, NC). Recombinant human vascular endothelial growth factor, VEGF 165, was from R&D systems (Minneapolis, MN). Human umbilical vein endothelial cells (HUVECs) and endothelial growth medium (EGM) were obtained from Lonza (Basel, Switzerland).

Radiolabeling of IgG Molecules

Bovine immunoglobulin G (IgG; purity≥95%) was dissolved in phosphate buffer saline (PBS; pH 7.4) to a final concentration of 1 mg/mL. Four Iodination-beads were submerged in excess PBS and allowed to incubate for 5 min. The PBS was removed from the vial containing the Iodination-beads and 1 mCi of ^{125}I mixed with 1 mL of IgG solution was added to the Iodination-beads. The iodination reaction was allowed to proceed for 15 min with periodic agitation. Subsequently, the Iodination-beads were removed and the reaction solution was dialyzed against fresh PBS for 24 h to remove any unincorporated ^{125}I.

Synthesis and Characterization of Degradable Cross-Linker

The synthesis of Acry-PLLA-*b*-PEG-*b*-PLLA-Acry cross-linker has been described in detail previously (5,18). In brief, 10 g of anhydrous poly(ethylene glycol) (PEG; average M_n = 3,350 Da) were combined with 2.1 g of anhydrous 3,6-dimethyl-1,4-dioxane-2,5-dione (l-lactide) over the catalyst Tin(II) 2-ethylhexanoate (Stannous Octoate; purity ~ 95%). The ring-opening polymerization was allowed to proceed over Argon (Ar) atmosphere for 4 h at 150°C. The triblock macromer product, PLLA-*b*-PEG-*b*-PLLA, was cooled and dissolved in 15 mL of dichloromethane (DCM; anhydrous, purity ≥ 99.8%) and filtered (Whatman glass microfiber filters; Kent, United Kingdom). The product was then precipitated in 500 mL of ice-cold diethyl ether (ether; anhydrous, purity ≥ 99.7%), dried, and redissolved in 15 mL of DCM. Precipitation was repeated one more time to ensure complete removal of stannous octoate and other impurities. The precipitate was dried and lyophilized for 24 h.

The PLLA-*b*-PEG-*b*-PLLA was end-capped with acrylate groups. Acryloyl chloride (Acry-Cl, 97%) and PLLA-*b*-PEG-*b*-PLLA were combined in a 10:1 molar ratio and dissolved in ~ 125 mL of dichloromethane. Triethylamine (TEA; 99%), at 1 to 12 molar ratio of TEA to PLLA-*b*-PEG-*b*-PLLA was first dissolved in ~ 15 mL of DCM. The TEA solution was gradually added to the PLLA-*b*-PEG-*b*-PLLA/Acry-Cl mix over vigorous agitation and the acrylation reaction proceeded overnight at room temperature under an Ar atmosphere. The product, Acry-PLLA-*b*-PEG-*b*-PLLA-Acry, recovered in a separation funnel was purified by three consecutive dissolution and precipitation procedures as described in the previous paragraph.

^{1}H NMR (Bruker 300; Bruker Corporation, Billerica, MA) analysis was performed on the synthesized Acry-PLLA-*b*-PEG-*b*-PLLA-Acry dissolved in deuterated chloroform. The number of lactic acid groups and the percent acrylation of the final triblock macromer were determined from the NMR data.

Hydrogel Polymerization

All solutions used to make the hydrogels were degassed by sonication before polymerization. The monomer N-isopropylacrylamide (NIPAAm; 97%) was dissolved in PBS buffer to a final concentration of 350 mM. ^{125}I-IgG (or Avastin® or Lucentis®) was added to a final concentration 0.1 mg/mL. L-glutathione (glutathione; purity ≥ 98.0%) was added at three different concentrations (0 mg/ml, 0.5 mg/mL and 1.0 mg/mL). The cross-linking macromer Acry-PLLA-*b*-PEG-*b*-PLLA-Acry was dissolved to a final concentration of 3 mM. Hydrogels were polymerized by free radical initiation in aqueous media with 13 mM ammonium persulfate (APS; purity ≥ 98%) as the initiator and 168 mM N,N,N′,N′-tetramethylethylenediamine (TEMED; purity = 98%) as the accelerator. Prior to mixing into the hydrogel precursors, the pH of TEMED solution was adjusted to 7.4 with hydrochloric acid. The volume of all hydrogels was 200 μL. All solutions were maintained at ~ 7°C before and during the polymerization. Free radical polymerization was allowed to proceed for 1 h. Formation of cross-linked hydrogels containing encapsulated proteins is depicted in Scheme 1. Monomer conversion was determined as the weight of dry hydrogel after extraction of salts, TEMED, and unreacted monomer divided by the weight of the initial dry monomers and cross-linkers.

Thermo-responsiveness Characterization

The effect of composition on the VPTT of the hydrogels was determined by optical absorption spectroscopy using a temperature controlled UV–vis plate reader (Molecular Devices SPECTRA Max Plus, Sunnyvale, CA) (19). The temperature of the samples was increased from 25°C to 43°C at 0.5°C increments. At each temperature increment step the samples were allowed to equilibrate for 15 min before absorbance measurements were taken. VPTTs were defined as the temperature at which 50% of the maximum absorbance change occurred.

Hydrogel Swelling

Hydrogel swelling ratios were measured to determine the change in hydrogel volume as a function of degradation time. The synthesized hydrogels were submerged in PBS at 37°C. At defined periods of time (initially hourly and later daily time intervals), the hydrogels were removed from the PBS and weighted. Prior to weight measurements, excess water on the surface of the hydrogels was removed by gentle vacuum aspiration through a metallic mesh and the weight of swollen hydrogel was obtained, $W_{swollen}$. The dry weight of each hydrogel, W_{dry}, was obtained after drying under vacuum at 80°C for 5 days. The hydrogel swelling ratio (Q) was calculated as the ratio of water weight to that of dry hydrogel weight:

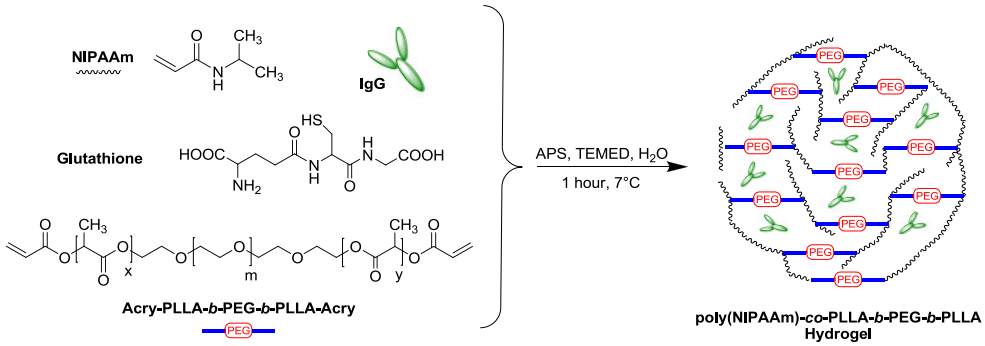

Scheme 1 Synthetic scheme of PNIPAAm-*co*-PLLA-*b*-PEG-*b*-PLLA hydrogels formation. The hydrogels consist of poly(N-isopropylacrylamide) (〰), poly(ethylene glycol) ((PEG)), poly(L-lactic Acid) (▬) and the encapsulated immunoglobulin G (). Idealized hydrogel structure is not-to-scale.

$$Q = \frac{W_{swollen} - W_{dry}}{W_{dry}} \quad (1)$$

PEGylation

PEGylation of IgG molecules was carried out at protein to PEGylation reagent ratios of 1:0 (control), 1:5, and 1:15. PEGylation buffer was prepared using 50 mM sodium bicarbonate adjusted to pH 8.7. For the 1:5 PEGylation ratio, 1 mL of 0.013 mM ^{125}I-IgG and 1 mL of 0.067 mM Acry-PEG-SVA dissolved in the $NaHCO_3$ buffer were prepared separately. Similarly, for the 1:15 PEGylation ratio, 1 mL of 0.013 mM ^{125}I-IgG and 1 mL of 0.201 mM Acry-PEG-SVA dissolved in the $NaHCO_3$ buffer solutions were prepared separately. Next, the ^{125}I-IgG and Acry-PEG-SVA were combined over gentle agitation. PEGylation was allowed to proceed in the dark for 2 h. The reaction product Acry-PEG-IgG was dialyzed against PBS for 24 h. IgG PEGylation is depicted in Scheme 2. SDS-PAGE was used to determine IgG PEGylation. Each PEGylated IgG sample was mixed with 45% v/v laemmli buffer and 9% v/v β-mercaptoethanol (BME). The proteins were further denatured by boiling the samples at 100°C for 5 min. Samples were cooled, loaded, and separated by size in the presence of the running buffer using XCell SureLock™ Mini-Cell electrophoresis apparatus (Invitrogen; Carlsbad, CA). Subsequently, the polyacrylamide gel was stained and fixed using acetic acid (99.7%).

Protein Release and Detection

For protein release experiments, hydrogels were transferred into individual 15 mL plastic vials (after extraction of unreacted monomer and initiator) and 5 mL of 37°C PBS were added to each vial. The hydrogels were incubated for up to 15 days at 37°C. Supernatant samples were collected at various time intervals in order to determine protein release. For this purpose, 0.2 mL supernatant samples were collected at given time intervals for the first 12 h of protein release. Subsequent samples were taken daily. The collected samples were replaced with 0.2 mL of fresh PBS. ^{125}I-IgG concentration in the samples was quantified by gamma radiation emitted and a mass balance was performed to determine the quantity remaining in the hydrogel. The idealized hydrogel structure during protein release experiments is portrayed in Scheme 3.

Cytotoxicity and Encapsulation Efficiency

Right after polymerization the hydrogels were subject to five consecutive buffer extraction procedures in order to remove cytotoxic components (e.g. unreacted monomers). Extractions consisted of gentle agitation of the hydrogels in excess PBS buffer at room temperature (1:25 volume ratio) for 20 min each. The extracts were not diluted, and 50 µl of the extract were added directly to the cells in 96 well plates in order to test toxicity. No attempt was made to determine toxic concentrations of the extracts since varying concentration of extracts has little relevance to the scope of our study because no cells will be exposed to the extract *in vivo*. Sodium azide (NaN_3; 0.05% w/v) was added to the PBS to prevent bacterial contamination during *in vitro* degradation experiments but was omitted when the hydrogels or its extracts were tested for cytotoxicity testing. A gamma counter (Packard BioScience CobraII Auto-Gamma; Meridian, CT) was used to measure radiation emitted by the ^{125}I-IgG in extracts and a mass balance was performed to calculate encapsulation efficiency.

3T3 fibroblast cells were seeded in T-75 flasks and cultured using complete growth medium (DMEM, 10% v/v FBS, and 1% v/v penicillin/streptomycin), in a 5% CO_2 atmosphere at 37°C. The growth medium was changed every 2–3 days. Cells were grown to confluence and harvested with trypsin/ethylenediaminetetraacetic acid (EDTA) solution. The cells were then suspended in growth medium and seeded in 96-well plates at 5,000 cells/well (200 µl) to allow cell adhesion for 3 h before adding the extractions (50 µl, without dilution). PBS was used as control group. An MTS assay was performed to determine cell viability after 2 days of exposure to testing

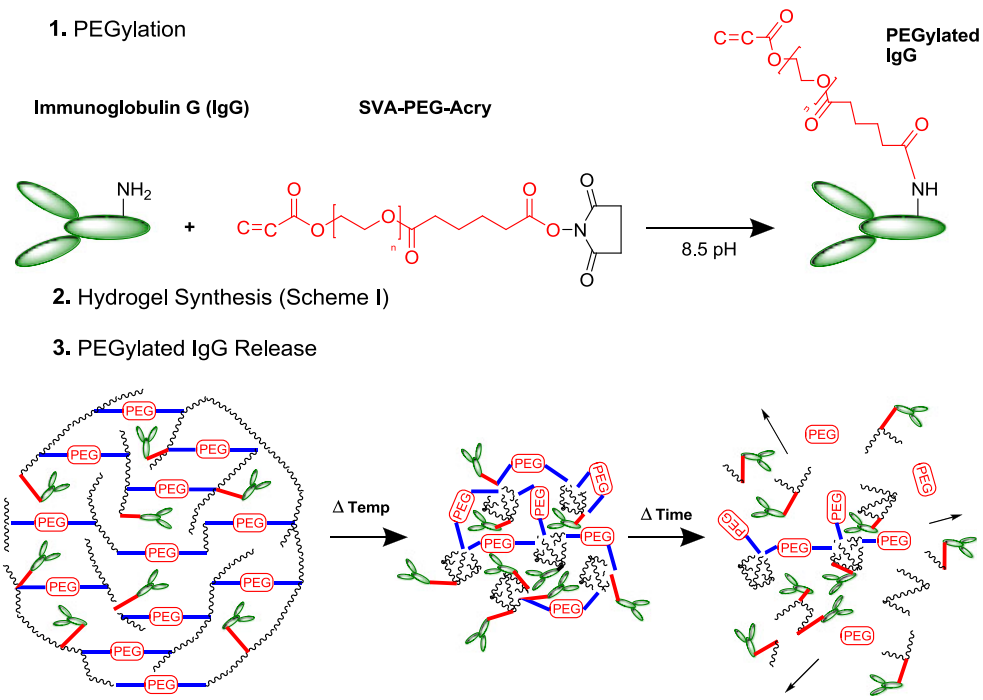

Scheme 2 (**1**) Schematic of IgG PEGylation using SVA-PEG-Acry reagent (▬). (**2**) Subsequent hydrogel synthesis and (**3**) release of IgG-PEG conjugate due to hydrogel degradation in the hydrophobic collapsed state at 37°C.

agents. The results were normalized to the absorbance observed in the PBS control.

Bioactivity of Avastin® and Lucentis®

HUVECs were cultured with EGM under the same conditions as 3T3 fibroblasts. Prior to addition of cells, 96-well plates were coated with 2.5 µg/ml fibronectin in HBSS to enhance cell adhesion. HUVECs were harvested and seeded at 5,000 cells/well in EGM (200 µl). The cells were incubated at 37°C under a 5% CO_2 humidified atmosphere for 3 days. Next, the EGM was removed and replaced with 200 µl/well of endothelial basal medium (EBM, Lonza) with 0.5% v/v FBS. The cells were then incubated for additional 24 h before adding test samples, including Avastin®/Lucentis®, PEGylated samples or release samples with 10 ng/ml VEGF. After 2 days of sample exposure, HUVEC proliferation was assessed with a BrdU ELISA assay. Exposure to FBS was used as the positive control group and PBS as a negative control.

Statistical Analysis

All data are expressed as mean ± standard deviation. For MTS cell toxicity assay and BrdU ELISA cell proliferation assay, one way ANOVA with a Tukey-Kramer post test was used for comparison among groups. Values of $p < 0.05$ were considered statistically significant.

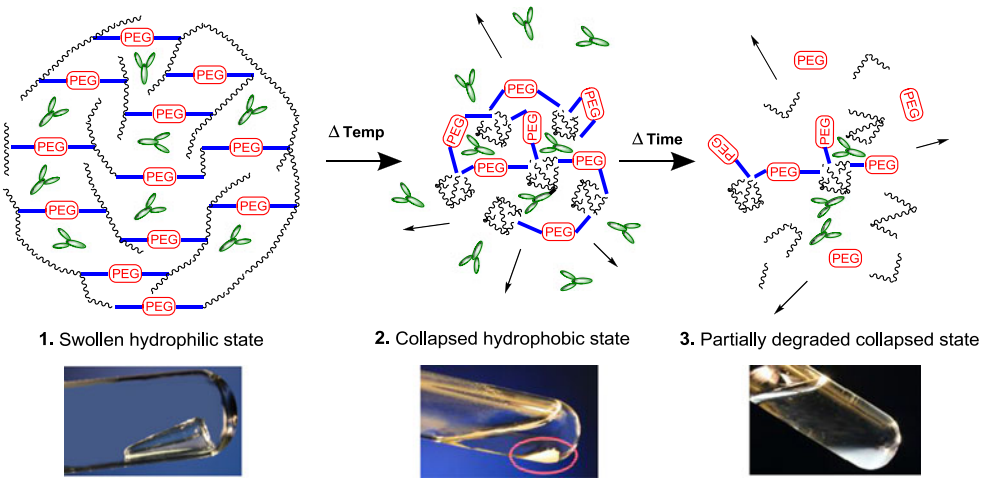

Scheme 3 Idealized structure and images of PNIPAAm-*co*-PLLA-*b*-PEG-*b*-PLLA hydrogels: (**1**) Post-synthesis swollen state at 7°C, below the VPTT (**2**) Collapsed state in buffer at 37°C, above the VPTT (**3**) After partial degradation through hydrolysis of the PLLA (▬) linkages in the collapsed state at 37°C.

RESULTS

Macromer Synthesis

^{1}H NMR analysis was performed on the synthesized Acry-PLLA-*b*-PEG-*b*-PLLA-Acry and Acry-PEG-Acry macromers and the results were as follows, ^{1}H-NMR ($CDCl_3$): 3.6 ppm (s, 174.43 H, PEG), 5.2 ppm (m, 4.93 H, CH_3-C<u>H</u>-), 5.9 ppm (d, 1.01 H, <u>H</u>-(CH)=C-), 6.2 ppm (m, 1.01 H, CH_2=C<u>H</u>-COO-), 6.5 ppm (d, 1.00 H, H-(C<u>H</u>)=C-), 1.5 (d, C<u>H</u>$_3$-CH-). The number of lactide monomers per mole of PEG macromer was calculated to be 8.3 ± 0.1. The percent acrylation of the final triblock macromer was $86.0 \pm 1.0\%$ and the average MW of Acry-PLLA-*b*-PEG-*b*-PLLA-Acry was 4,120 Da. ^{1}H-NMR of Acry-PLLA-b-PEG-b-PLLA-Acry macromere is available in Supplementary Material.

Hydrogel Characterization

Table I shows swelling ratio, conversion, transition temperature (VPTT), and protein encapsulation efficiency of hydrogels prior to *in-vitro* IgG release. The initial swelling ratios, $Q_{t=0}$, at 7°C increased with glutathione concentration. The VPTT values ranged from 32.5°C to 35.0°C. The VPPTs for all cross-linked hydrogels were higher than the lower critical solution temperature (LCST) of pure PNIPAAm (ca. 32°C) (20). Monomer conversion was found to be high (85–99%) as previously reported for similar NIPAAm polymerization systems where glutathione was not used (19,21).

Cytotoxicity and Encapsulation Efficiency

Following the 1-hour polymerization period, unreacted monomer and initiators were removed by five consecutive PBS buffer extraction procedures, which could also result in extraction of encapsulated proteins. Figure 1a shows that the removal of encapsulated protein during buffer extraction steps was small. After five extraction steps, about 75–85% of encapsulated protein was retained within the hydrogels. The MTS cytotoxicity assay showed that the relative survival of 3T3 cells increased with each buffer extraction procedure (Fig. 1b). The first buffer extract was the most toxic with a statistically significant drop in cell proliferation as compared to PBS control ($p < 0.05$). The mean encapsulation efficiencies (Table I) for the degradable hydrogels were 86, 83 and 75.3% for 0, 0.5 and 1.0 mg/mL CTA hydrogels respectively.

Degradation Behavior

Figure 2 shows the effect of glutathione on the degradation behavior of hydrogels. Hydrogels were incubated at 37°C and the swelling ratio (Q) measured as a function of time. As the hydrogels are submerged in PBS at 37°C, the swelling ratios dropped during the first hours of incubation. Glutathione containing hydrogels crosslinked with PNIPAAm-*co*-PLLA-*b*-PEG-*b*-PLLA completely degraded in 3 and 12 days. As the degradation proceeds, the swelling ratios increase and then rapidly approach infinite values when the hydrogels fully disintegrate. Hydrogels without CTA did not show evidence of disintegration within the 15 day timeframe at 37°C.

Release of IgG Molecules

Figure 3 shows the release of IgG molecules from degradable hydrogels with varying glutathione concentration. IgG released as the hydrogels degraded, thus the release rate was closely co-related with hydrogel degradation rate. The proteins completely released at day 3 and day 10 for hydrogels with 1 mg/ml and 0.5 mg/ml glutathione, respectively. Hydrogels without CTA only showed about 60% protein release at day 14.

Controlling Burst Release by PEGylation of IgG

Burst release occurred in all protein release profiles presented. For instance, for degradable hydrogels with 0.5 mg/mL glutathione CTA, approximately 60% of the encapsulated protein was released from the hydrogel in the first 24 h (Fig. 3). In order to reduce burst release, the IgG molecules were PEGylated using ratios of Acry-PEG-SVA to IgG of 1:0 (control), 1:5 and 1:15. SDS-PAGE was used to confirm the molecular weight change in the IgG protein. After the tetrameric quaternary structure of IgG was denatured using standard SDS-PAGE procedure, the resulting peptides were separated by size. PEGylation of IgG was confirmed as a discreet pattern of bands in the heavy chains of the PEGylated IgG (Fig. 4).

The protein release kinetics of PEGylated IgG were obtained at fixed concentration of glutathione CTA of 0.5 mg/ml. Figure 5 shows a clear shift in the burst release behavior. Compared to the control, IgG PEGylated with at 1:15 ratio of antibody to PEG-Acry caused an approximate 12-fold drop in burst release. Similarly, IgG PEGylated with at 1:5 ratio of antibody to PEG-Acry resulted in 3-fold decrease of burst behavior. After the initial hydrogel collapse, a very small and almost constant rate of release was observed for approximately 8 days. After this time, the release profiles of degradable hydrogels began to sharply diverge as the PNIPAAm chains disassociated from one another and the hydrogel disintegrated. Over 60% of the encapsulated protein was release between the 9th and 10th day. These results indicate that PEGylation of IgG is a viable method for delaying the burst release from degradable hydrogels.

Table I Characteristics of PNIPAAm-*co*-PLLA-*b*-PEG-*b*-PLLA Hydrogels at Varying Concentrations of Glutathione CTA

Crosslinker	[glutathione] (mg/ml)	[a]Initial swelling ratio $Q_{t=0}$	VPTT (°C)	Monomer conversion (%)	% Encapsulation efficiency of IgG
Acry-PLLA-b-PEG-b-PLLA-Acry	0	23.9 ± 1.6	32.9 ± 0.7	95.9 ± 2.3	86.5 ± 1.0
	0.5	34.7 ± 4.4	34.1 ± 0.2	97.2 ± 1.8	80.1 ± 3.4
	1.0	37.4 ± 5.4	35.0 ± 0.6	84.9 ± 3.9	75.3 ± 2.5

Values were measured after buffer extractions and prior to IgG release ($n = 3$)

[a] At room temperature after extraction procedures and equilibration in buffer overnight

Bioactivity of Released Molecules

In order to determine the bioactivity of encapsulated PEGylated Avastin® and Lucentis® (1:5 molar ratio of protein to Acry-PEG-SVA) hydrogels made with 0.5 mg/mL CTA and 3 mM Acry-PLLA-b-PEG-b-PLLA-Acry were incubated at 37°C until they became completely soluble and hence, released all of the encapsulated molecules. These hydrogels disintegrated completely in about 8–9 days. Since the potential toxicity of degradation products could mask the effects of angiogenesis inhibition, the cytotoxicity of hydrogel degradation products was evaluated first. Hydrogel degradation products did not exhibit cytotoxicity as compared to the PBS control and the differences were not statistically significant ($p > 0.05$) (Supplementary Material). The released molecules were tested for their ability to inhibit VEGF-stimulated cell growth. Figure 6 shows the results of the BrdU assay results. All samples were tested in the presence of VEGF (10 ng/ml). Both Avastin® and Lucentis® reduced the effect of VEGF on cell proliferation. Inhibition of HUVEC growth due to bulk Avastin® and Lucentis® was statistically significant ($p < 0.001$) as compared to VEGF without angiogenesis inhibitors. This is expected because at 1 mg/mL, the antibody concentrations were higher than established clinically-active doses (0.25 mg/mL for Avastin® and 0.125 mg/mL for Lucentis®) (22). Statistically significant differences in cell proliferation between bulk Avastin® and bulk Lucentis® were also observed. It has been reported that Avastin® is bioactive in VEGF neutralization at 1 μg/mL whereas the threshold for Lucentis® bioactivity is 60 ng/mL (23). The 17-fold higher VEGF binding capacity of Lucentis® compared with Avastin® may explain the difference in inhibition of HUVEC proliferation.

DISCUSSION

The ^{1}H-NMR of Acry-PLLA-*b*-PEG-*b*-PLLA-Acry was in agreement with the expected chemical structure. This macromere had about eight degradable lactate units per molecule and its acrylation was high. This is consistent with previously reported values for the synthesis of this tri-block macromer (5,18).

The addition of glutathione (CTA) resulted in larger initial swelling ratios for all hydrogels, which is expected since CTAs limit chain propagation. By reducing the total amount of cross-links that can be established in the hydrogel the molecular weight between crosslinks is increased (24). For neutral and highly swollen hydrogels ($Q \geq 10$), the relationship

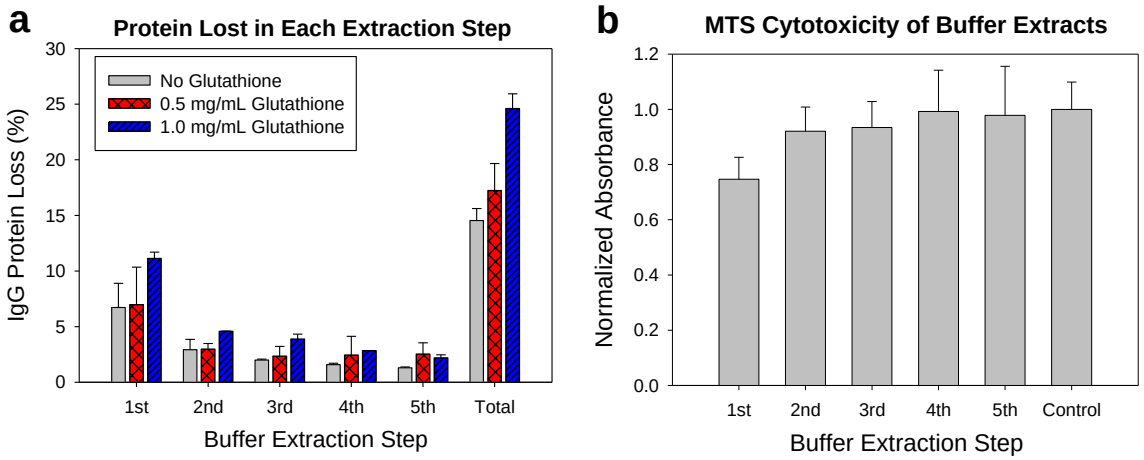

Fig. 1 (**a**) IgG protein loss and (**b**) corresponding MTS cytotoxicity of post-polymerization buffer extracts used to remove unreacted monomers and free radical initiators of PNIPAAm-*co*-PLLA-*b*-PEG-*b*-PLLA hydrogels ($n = 3$).

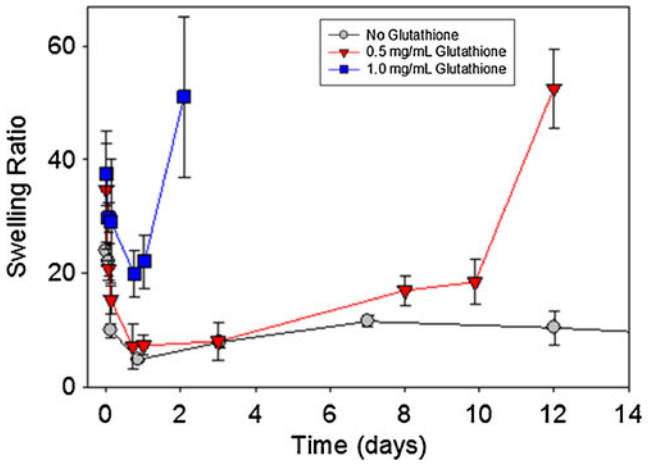

Fig. 2 Volumetric swelling ratios at 37°C as a function of degradation time for hydrogels polymerized with varying glutathione CTA concentrations ($n = 3$).

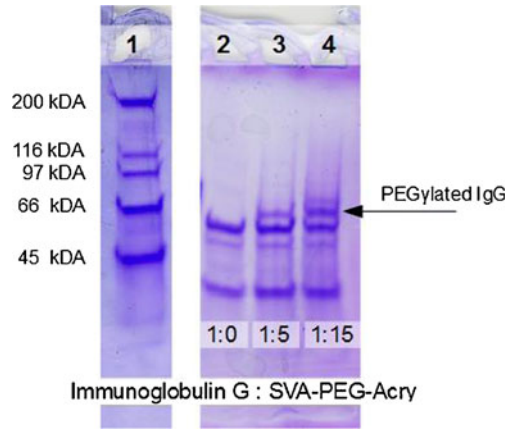

Fig. 4 SDS-PAGE analysis of IgG PEGylation. Lane 1: molecular weight marker. Lane 2: No PEGylation control IgG. Lane 3: IgG PEGylated at 1 to 5 M ratio of IgG to Acry-PEG-SVA. Lane 4: IgG PEGylated at 1 to 15 M ratio of IgG to Acry-PEG-SVA.

between swelling ratio, Q, and molecular weight is simplified as equation (2):

$$Q = \left(\frac{\bar{v}\left({}^{1}/_{2} - 2\chi_{12}\right)\overline{M}_c}{V_1}\right)^{3/5} = \beta\left(\overline{M}_c\right)^{3/5} \qquad (2)$$

where $\bar{v}$ is the specific polymer volume, V_1 the molar volume of water, and χ_{12} the polymer-water interaction parameter (25,26,27). These parameters can be lumped into a single constant (β) and depend little on CTA concentrations. Thus, swelling ratios scale with $\left(\overline{M}_c\right)^{3/5}$.

The hydrogels reported here were all capable of being injected through a 30-gauge needle at room temperature (15). Characterizing the thermo-responsive behavior of hydrogels is important because the phase transition that causes a change in the consistency of the hydrogel, from a predominantly viscous material that can be forced through a needle, to a viscoelastic solid at 37°C, is of critical importance for localized drug delivery. The VPPTs for all cross-linked hydrogels were higher than the lower critical solution temperature (LCST) of pure PNIPAAm (ca. 32°C) (20). This is due to the hydrophilic PEG, which elevates the VPTT (19,28). The increase in VPTT upon addition of CTA could be due to the incorporation of polar groups (amine and carboxyl) from glutathione during chain transfer. Also, polar groups incorporated within smaller PNIPAAm chains have more influence in changing the transition temperature (29). CTAs can make the hydrogels more heterogeneous because chain transfer increases polymer polydispersity and will also introduce polar amine and carboxyl groups from glutathione into the polymer chains (24). As a result, the hydrophilic/hydrophobic balance of heterogeneous hydrogels will differ across the volume of the material. This difference might explain the increase in VPTT

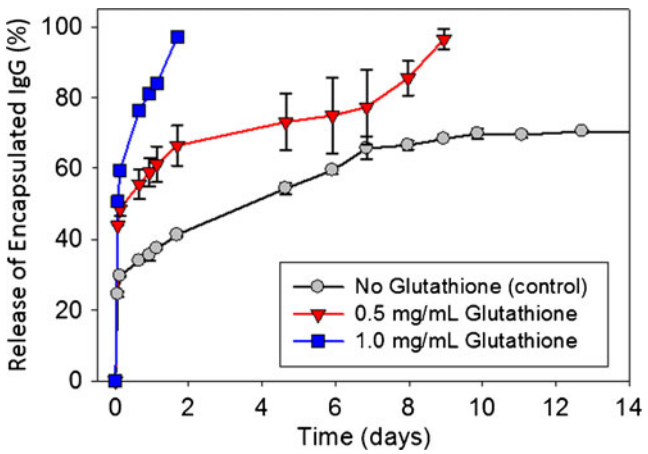

Fig. 3 IgG release at 37°C as a function of degradation time for hydrogels polymerized with varying glutathione CTA concentrations ($n = 3$).

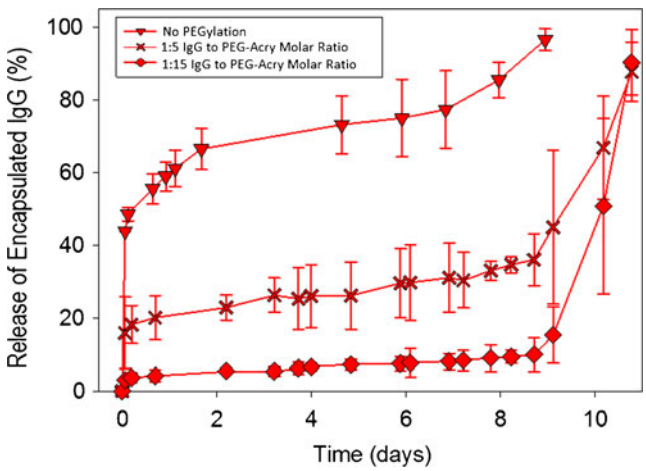

Fig. 5 Release at 37°C as a function of degradation time for IgG with varying degree of PEGylation: No PEGylation (▽), IgG PEGylated at 1 to 5 M ratio of IgG to Acry-PEG-SVA (✕), and IgG PEGylated at 1 to 15 M ratio of IgG to Acry-PEG-SVA (◆). The CTA concentration was fixed at 0.5 mg/mL glutathione.

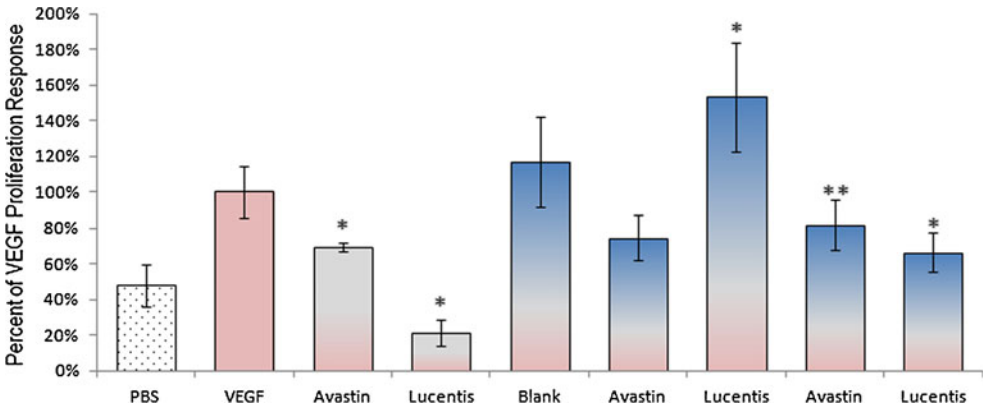

Fig. 6 BrdU assay results of HUVEC proliferation. PBS is the negative control. All other samples were cultured in the presence of VEGF (10 ng/ml). Thermo-responsive PNIPAAm-co-PEG-b-PLLA hydrogels were used for encapsulation and release of Avastin® or Lucentis®. The sample named "Blank" consists of the extracts of hydrogels without encapsulated molecules. Statistical analysis was performed using ANOVA. (standard deviation bars, $*p < 0.001$ *vs*. VEGF, $**p < 0.05$ *vs*. VEGF).

and the wider range of temperatures for the phase transition upon addition of glutathione CTA (Supplementary Material).

The toxicity of acrylamides is well-documented (30) and free radical initiators can cause oxidative damage to cells (31). Because the presence of unreacted monomers and initiators in the hydrogel are undesirable, it was necessary to remove unreacted materials from the hydrogels using buffer extraction. A minimum of three PBS buffer extractions were needed to remove cytotoxic elements from the hydrogels (Fig. 1b). During these extraction procedures a portion of the encapsulated IgGs were also removed. Glutathione had no bearing on cytotoxicity. However, addition of CTAs significantly increased the amount of IgG lost during the extractions. This likely resulted from the decreased cross-link density of the hydrogels at higher CTA concentrations.

The swelling ratios of hydrogels decreased quickly during the first hours of incubation at 37°C. This drop is due to dehydration and collapse of the PNIPAAm chains. Below the VPTT, the hydrogels are dominated by hydrophilic water-polymer interactions characterized by high swelling ratios. These interactions occur because water molecules form hydrogen bonds with pendant amide groups in PNIPAAm. As the temperature increases, water-polymer hydrogen bonds weaken and the hydrophobic interactions of PNIPAAm's nonpolar backbone and pendant isopropyl groups start to dominate and hydrogels dehydrate above the VPTT. Interestingly, these results indicate that at least 12 h are needed for the hydrophilic/hydrophobic transition to fully collapse the hydrogels at 37°C. Because of the time scale for this process, this time delay is likely due to kinetics of polymer chain transitions during the collapse of the hydrogels rather than heat transfer effects.

Hydrogels prepared with CTA completely disintegrated after enough incubation times in buffer at 37°C (Figs. 2 and 3). However, when CTA was not used the hydrogels did not disintegrate even if the crosslinker was degradable. We speculate that in degradable hydrogels prepared without CTA longer PNIPAAm chains in the collapsed state act as physical cross-links by means of hydrophobic interactions. In fact, when they were incubated at 37°C for sufficiently long times to degrade the Acry-PLLA-*b*-PEG-*b*-PLLA-Acry cross-links, they disintegrated immediately when brought back to room temperature (below their VPPT). This indicates that the lactate groups in the cross-links were actually hydrolyzed but the material would not fall apart because the collapsed PNIPAAm chains kept the material together through physical crosslinks (due to hydrophobic interactions).

In order to explain how CTAs facilitate hydrogel disintegration it is necessary to consider what happens to the PNIPAAm chains after hydrolysis of the Acry-PLLA-*b*-PEG-*b*-PLLA-Acry cross-links. Hydrolysis of the lactate units results in PNIPAAm chains bearing carboxylic acid moieties (Scheme 4). These increase the hydrophilic character of the resulting PNIPAAm chains thus shifting their transition point to higher temperatures. This change is in addition to the increased hydrophilicity due to CTA. Since the hydrogels prepared with CTA show VPPTs below 37°C before degradation we speculate that the additional increase in hydrophilicity by carboxylic acid moieties due to cross-linker degradation may further shift the transition temperature of degraded polymer chains above 37°C. This causes their dissolution and contributes to hydrogel disintegration. We found out that the transition temperature of hydrogel degradation products was above 45°C, which is the limit of the heating stage used for these measurements. In fact, the degradation products appeared translucent and did not show much opacity at 37°C (in contrast to linear PNIPAAm chains where the solution turns significantly turbid above the LCST of 32°C). This indicates a significant number of PNIPAAm chains of the degraded hydrogel had transition temperatures above physiological temperature. The significance of this change in transition temperature upon hydrogel degradation is that it could

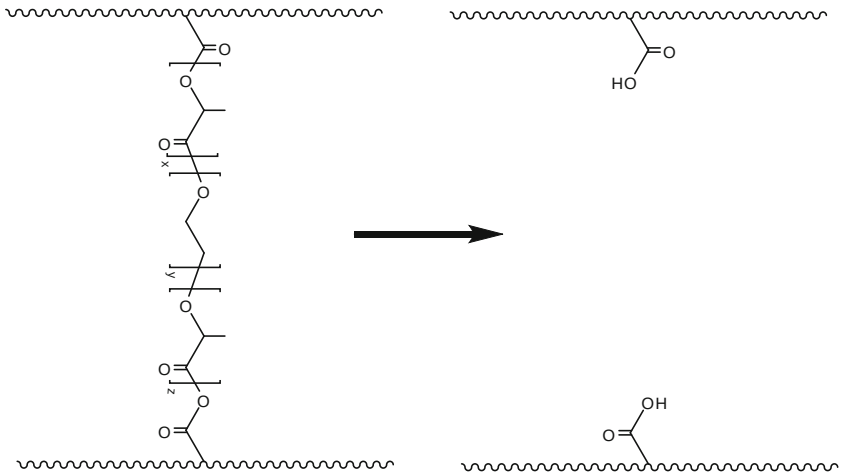

Scheme 4 Hydrolysis of the degradable cross-linker Acry-PLLA-PEG-PLLA-Acry results in hydrophilic carboxyl groups in the PNIPAAm chains. This increase in hydrophilic character of the PNIPAAm chains upon hydrolysis of the cross-linker can shift the VPPT of the degraded material to higher temperatures.

be advantageously exploited to facilitate clearance of PNIPAAm upon hydrogel degradation (17,32).

The degradation and release kinetics shows a plateau-like region occurring after the initial burst release and that after this plateau there is a quick change in the kinetics right before the disintegration of the hydrogel (Figs. 2 and 3). Degradation of hydrogels cross-linked with PLLA-*b*-PEG-*b*-PLLA is characterized by two distinct phases (33,34). In the first phase, degradation is governed by first-order hydrolysis of ester bonds in PLLA as expressed in the following equation:

$$\frac{d[E]}{dt} = -k_{H^+}[E][H_2O][H^+] - k_{OH^-}[E][H_2O][OH^-] \qquad (3)$$

were, t is degradation time, k_{H^+} and k_{OH^-} are acid and base catalyzed hydrolysis reaction rate constants, $[E]$ the ester concentration in PLLA, $[H_2O]$, $[H^+]$, and $[OH^-]$ are water, proton, and hydroxide concentrations. Water, proton and hydroxide concentrations do not change at constant pH in buffer. Integrating Eq. 3, noting that $[E]$ is inversely proportional to $\overline{M}_c$, and combining with Eq. 2 show that the volumetric swelling ratios would scale with degradation time according to the relationship $Q \sim e^{k_1 t}$ (26,35). This relationship explains the exponential increase in Q observed in Fig. 2 after the initial collapse/deswelling regime and explains why swelling ratios increase with degradation time after the initial collapse for degradable hydrogels.

It is worth noticing that the final degradation exhibits a sharp increase in Q over a short period of time. As the ester hydrolysis and breakdown of PLLA cross-links proceeds, there comes a point when individual PNIPAAm chains escape from the rest of the hydrogel matrix. At this point, the entire polymer structure dissolves (depending on transition temperature of the degradation products). If the degraded polymer chains are above the transition temperature, the physical cross-links formed by hydrophobic interactions of PNIPAAm prevent complete disintegration irrespective of the degree of PLLA ester hydrolysis. This is the case for degradable hydrogels prepared without addition of CTA during polymerization. The results in Fig. 2 indicate that addition of CTA during hydrogel formation help achieve solubility of degraded thermo-responsive hydrogels above 37°C and that glutathione can be used as means to control the rate of hydrogel degradation.

The initial burst release of encapsulated IgG is most likely caused by convective mass transport of proteins within and away from them. Convective mass transport results from the bulk fluid motion induced during deswelling (collapse) of the hydrogels as the VPTT was reached. During deswelling, the cross-linked structure alters shape, creates internal stresses, and the resulting convection of fluid helps release the encapsulated protein. This could help explain the dependence of burst release amounts as a function of crosslinking agent (which is observed to significant extents even after the extraction procedures removed surface bound and untrapped molecules). For less crosslinked hydrogels (more CTA) the induced fluid motion during chain collapse is more prominent because of an initially more open structure.

The IgG release behavior from these hydrogels appears to be controlled in part by the changing cross-link density because the overall shape of IgG release profiles resembles the swelling ratios as a function of degradation time. This is expected since the diffusion coefficient of drugs within the cross-linked hydrogel are a function of mesh size (which determines swelling ratios), and the size of the biomolecule (27). Also, the disintegration of the hydrogels leads to complete release of the encapsulated molecules. The most significant finding in Figs. 2 and 3 is that the IgG release can be controlled by glutathione CTA addition because glutathione decreases the cross-link density and elevates the swelling ratios of thermo-responsive hydrogels in the collapsed state.

Burst release can be undesirable because it may limit the effectiveness of a drug delivery system. To counteract this behavior, tethering of IgG by PEGylation and subsequent covalent attachment to the hydrogel was investigated. The PEG to

protein molar ratio is important in the PEGylation of therapeutic proteins. Higher ratios of Acry-PEG-SVA to IgG will make it easier to attach the protein to the hydrogel. However, this can diminish activity if the PEG blocks the antigen binding sites. A 1:15 ratio of antibody to PEG has been reported as the upper limit to preserve biological activity (36). In this study, Acry-PEG-SVA to IgG ratios were: 1:0 (control), 1:5 and 1:15. Successful PEGylation was confirmed by SDS-PAGE, which shows bands of the Fc fragment with increased molecular weight (Fig. 4). Within the limits of detection provided by SDS-PAGE there was no evidence of significant PEGylation of the F_{ab} regions of IgGs. Thus, it is likely that the biological activity of the encapsulated molecules is maintained because the antigen binding sites (F_{ab} regions) are not blocked with PEG tether. It should be noted however, that although PEGylation of IgGs helps eliminate the initial burst behavior, a delayed burst release is still observed (Fig. 5). Most likely this resulted because degradation of the PLLA regions is faster than that of the ester bond of the Acry-PEG-SVA tether. Thus, the tethered molecules are not released until the hydrogel disintegrates. This result could be useful when pulsed release was desired. For example, by administering compositions where the pulsed release would occur at different time points. The results also indicate the need to design PEG tethers with slightly faster degradation kinetics than the Acry-PLLA-b-PEG-b-PLLA-Acry crosslinkers in order to achieve sustained release.

Of greatest importance in validating the proposed drug delivery system is the bioactivity of encapsulated and released angiogenesis inhibitors. Released Lucentis® and Avastin®, whether PEGylated or not, showed statistically significant decreases in HUVEC proliferation compared to the VEGF control ($p < 0.05$). Cell growth was not affected by the presence of hydrogel alone. These results indicate that the hydrogels preserve the biological activity of anti-VEGF agents and that PEGylation, at molar ratios explored in this study, did not alter the activity of Avastin® and Lucentis® significantly. No statistically significant difference was observed between the released Avastin® and stock Avastin® solutions ($p > 0.05$). However, bulk Lucentis® appeared to be more effective at inhibiting VEGF signaling than Lucentis® released from the hydrogels ($p < 0.05$). These results may be due to differences in concentration of the two samples. Although care was taken to ensure the bulk and released Lucentis® concentrations were equivalent, a potentially higher amount of Lucentis® may have been lost during the buffer extraction procedure of hydrogel synthesis, possibly due to the smaller size of Lucentis® (48 kDa) compared with Avastin® (149 kDa) and IgG (150 kDa).

CONCLUSIONS

This work determined that CTAs and PEGylation can control the release kinetics of antibodies from degradable and thermo-responsive hydrogels composed of PEG, PLLA, and PNIPAAm. Hydrogels were synthesized *via* free radical polymerization either in the presence or absence of glutathione as CTA. At the molar concentrations explored in this study, glutathione was found to significantly change drug delivery properties of all hydrogels. Prior to *in vitro* release, hydrogels with glutathione exhibited higher swelling and lower encapsulation efficiency. In the collapsed state at 37°C, addition of glutathione was especially important for degradable hydrogels since it allowed solubilization of degradation products. Addition of 1.0 mg/mL CTA accelerated complete degradation to less than 2 days of incubation at 37°C; whereas hydrogels without glutathione CTA did not show evidence of degradation in over 3 weeks based on swelling ratio measurements.

Tethering of IgG through PEGylation and subsequent attachment to the polymer chains diminished burst release in the initial swelling phase of the release. In hydrogels with 0.5 mg/mL glutathione CTA, PEGylation resulted in over 3-fold drop in initial burst. The majority of PEGylated IgG was only released when the hydrogel began to disintegrate after *ca*. 10 days. This likely occurred because hydrolysis of the crosslinkers was faster than hydrolysis of the PEGylation moieties. Thus, it is possible that the delayed burst release could be controlled by designing PEGylation reagents that hydrolyze faster than the hydrogel crosslinkers. The bioactivity of encapsulated Avastin® and Lucentis® were retained whether these molecules were PEGylated or not. Thus, this system is promising for localized drug delivery applications in diseases such as wet age related macular degeneration.

ACKNOWLEDGMENTS AND DISCLOSURES

We would like to thank Chen Zhang and Michael Turturro for help with PEGylation and radiolabeling of IgG. This research was made possible through the funding provided by The Lincy Foundation, The Macula Foundation and the Veterans Administration.

REFERENCES

1. Linand CC, Anseth KS. PEG hydrogels for the controlled release of biomolecules in regenerative medicine. Pharm Res. 2009;26:631–43.
2. Oh JK, Drumright R, Siegwart DJ, Matyjaszewski K. The development of microgels/nanogels for drug delivery applications. Prog Polym Sci. 2008;33:448–77.
3. Peppas NA, Bures P, Leobandung W, Ichikawa H. Hydrogels in pharmaceutical formulations. Eur J Pharm Biopharm. 2000;50:27–46.
4. Peppas NA, Hilt JZ, Khademhosseini A, Langer R. Hydrogels in biology and medicine: from molecular principles to bionanotechnology. Adv Mater. 2006;18:1345–60.
5. Sawhney AS, Pathak CP, Hubbell JA. Bioerodible hydrogels based on photopolymerized poly(ethylene glycol)-co-poly(alpha-hydroxy acid) diacrylate macromers. Macromolecules. 1993;26:581–7.

6. Westand JL, Hubbell JA. Photopolymerized hydrogel materials for drug-delivery applications. React Polym. 1995;25:139–47.
7. Kloudaand L, Mikos AG. Thermo-responsive hydrogels in biomedical applications. Eur J Pharm Biopharm. 2008;68:34–45.
8. Ruel-Gariepyand E, Leroux JC. In situ-forming hydrogels—review of temperature-sensitive systems. Eur J Pharm Biopharm. 2004;58: 409–26.
9. Jeong B, Kim SW, Bae YH. Thermosensitive sol–gel reversible hydrogels. Adv Drug Deliv Rev. 2002;54:37–51.
10. Hoffman AS. Applications of thermally reversible polymers and hydrogels in therapeutics and diagnostics. J Control Release. 1987;6:297–305.
11. Donati G. Emerging therapies for neovascular age-related macular degeneration: state of the art. Ophthalmologica. 2007;221:366–77.
12. Fung AE, Lalwani GA, Rosenfeld PJ, Dubovy SR, Michels S, Feuer WJ, *et al*. An optical coherence tomography-guided, variable dosing regimen with intravitreal ranibizumab (lucentis) for neovascular age-related macular degeneration. Am J Ophthalmol. 2007;143:566–83.
13. Rosenfeld PJ. Intravitreal Avastin: the low cost alternative to lucentis? Am J Ophthalmol. 2006;142:141–3.
14. Bhatnagar P, Spaide Richard F, Takahashi Beatriz S, Peragallo Jason H, Freund KB, Klancnik James Jr M, *et al*. Ranibizumab for treatment of choroidal neovascularization secondary to age-related macular degeneration. Retina. 2007;27:846–50.
15. Turturro SB, Guthrie MJ, Appel AA, Drapala PW, Brey EM, Pérez-Luna VH, *et al*. The effects of cross-linked thermo-responsive PNIPAAm-based hydrogel injection on retinal function. Biomaterials. 2011;32:3620–6.
16. Mari M, Morales A, Colell A, Garcia-Ruiz C, Fernandez-Checa JC. Mitochondrial glutathione, a key survival antioxidant. Antioxid Redox Signal. 2009;11:2685–700.
17. Bertrand N, Fleischer JG, Wasan KM, Leroux J-C. Pharmacokinetics and biodistribution of N-isopropylacrylamide copolymers for the design of pH-sensitive liposomes. Biomaterials. 2009;30:2598–605.
18. Chiu Y-C, Larson JC, Perez-Luna VH, Brey EM. Formation of microchannels in poly(ethylene glycol) hydrogels by selective degradation of patterned microstructures. Chem Mater. 2009;21:1677–82.
19. Drapala PW, Brey EM, Mieler WF, Venerus DC, Derwent JJK, Pérez-Luna VH. Role of thermo-responsiveness and poly(ethylene glycol) diacrylate cross-link density on protein release from poly(N-isopropylacrylamide) hydrogels. J Biomater Sci Polym Ed. 2011;22: 59–75.
20. Schild HG. Poly (N-isopropylacrylamide) - experiment, theory and application. Prog Polym Sci. 1992;17:163–249.
21. Kaneko Y, Nakamura S, Sakai K, Aoyagi T, Kikuchi A, Sakurai Y, *et al*. Rapid deswelling response of poly(N-isopropylacrylamide) hydrogels by the formation of water release channels using poly(ethylene oxide) graft chains. Macromolecules. 1998;31:6099–105.
22. Costa R, Carneiro A, Rocha A, Pirraco A, Falcao M, Vasques L, *et al*. Bevacizumab and ranibizumab on microvascular endothelial cells: a comparative study. J Cell Biochem. 2009;108:1410–7.
23. Klettnerand A, Roider J. Comparison of bevacizumab, ranibizumab, and pegaptanib in vitro: efficiency and possible additional pathways. Investig Ophthalmol Vis Sci. 2008;49:4523–7.
24. Kricheldorf HR, Nuyken O, Swift G. Handbook of polymer synthesis. New York: Marcel Dekker; 2005.
25. Flory PJ. Principles of polymer chemistry. Ithaca: Cornell University Press; 1953.
26. Mason MN, Metters AT, Bowman CN, Anseth KS. Predicting controlled-release behavior of degradable PLA-b-PEG-b-PLA hydrogels. Macromolecules. 2001;34:4630–5.
27. Linand CC, Metters AT. Hydrogels in controlled release formulations: network design and mathematical modeling. Adv Drug Deliv Rev. 2006;58:1379–408.
28. Nolan CM, Reyes CD, Debord JD, Garcia AJ, Lyon LA. Phase transition behavior, protein adsorption, and cell adhesion resistance of poly(ethylene glycol) cross-linked microgel particles. Biomacromolecules. 2005;6:2032–9.
29. Furyk S, Zhang YJ, Ortiz-Acosta D, Cremer PS, Bergbreiter DE. Effects of end group polarity and molecular weight on the lower critical solution temperature of poly(N-isopropylacrylamide). J Polym Sci A Polym Chem. 2006;44:1492–501.
30. Friedman M. Chemistry, biochemistry, and safety of acrylamide. A review. J Agric Food Chem. 2003;51:4504–26.
31. Williams CG, Malik AN, Kim TK, Manson PN, Elisseeff JH. Variable cytocompatibility of six cell lines with photoinitiators used for polymerizing hydrogels and cell encapsulation. Biomaterials. 2005;26:1211–8.
32. Yamaoka T, Tabata Y, Ikada Y. Distribution and tissue uptake of poly(ethylene glycol) with different molecular-weights after intravenous administration to mice. J Pharm Sci. 1994;83:601–6.
33. Metters AT, Anseth KS, Bowman CN. A statistical kinetic model for the bulk degradation of PLA-b-PEG-b-PLA hydrogel networks: incorporating network non-idealities. J Phys Chem B. 2001;105:8069–76.
34. Metters AT, Anseth KS, Bowman CN. Fundamental studies of a novel, biodegradable PEG-b-PLA hydrogel. Polymer. 2000;41: 3993–4004.
35. Metters AT, Bowman CN, Anseth KS. A statistical kinetic model for the bulk degradation of PLA-b-PEG-b-PLA hydrogel networks. J Phys Chem B. 2000;104:7043–9.
36. Fipulaand D, Zhao H. Releasable PEGylation of proteins with customized linkers. Adv Drug Deliv Rev. 2008;60:29–49.